Talanta 115 (2013) 222–227

Contents lists available at ScienceDirect

Talanta

journal homepage: www.elsevier.com/locate/talanta

Molecularly imprinted electrochemical sensor based on amine group modified graphene covalently linked electrode for 4-nonylphenol detection

Hong-Jun Chen [a,b], Zhao-Hui Zhang [a,b,c,*], Rong Cai [b], Xing Chen [b], Yu-Nan Liu [b], Wei Rao [b], Shou-Zhuo Yao [c]

[a] *Key laboratory of Hunan Forest Products and Chemical Industry Engineering, Jishou University, Hunan 427000, PR China*
[b] *College of Chemistry and Chemical Engineering, Jishou University, Hunan 416000, PR China*
[c] *State Key Laboratory of Chemo/Biosensing and Chemometrics, Hunan 410082, PR China*

ARTICLE INFO

Article history:
Received 25 February 2013
Received in revised form
22 April 2013
Accepted 24 April 2013
Available online 3 May 2013

Keywords:
Molecularly imprinted
4-Nonylphenol
Graphene
Electrochemical sensor

ABSTRACT

In this work, an imprinted electrochemical sensor based on electrochemical reduced graphene covalently modified carbon electrode was developed for the determination of 4-nonylphenol (NP). An amine-terminated functional graphene oxide was covalently modified onto the electrode surface with diazonium salt reactions to improve the stability and reproducibility of the imprinted sensor. The electrochemical properties of each modified electrodes were investigated with differential pulse voltammetry (DPV). The electrochemical characteristic of the imprinted sensor was also investigated using electrochemical impedance spectroscopy (EIS) in detail. The response currents of the imprinted electrode exhibited a linear relationship toward 4-nonylphenol concentration ranging from 1.0×10^{-11} to 1.0×10^{-8} g mL^{-1} with the detection limit of 3.5×10^{-12} g mL^{-1} (S/N=3). The fabricated electrochemical imprinted sensor was successfully applied to the detection of 4-nonylphenol in rain and lake water samples.

1. Introduction

4-Nonylphenol (NP) has been considered as harmful to the reproductive health of human and wildlife since it has been designated as a member of the endocrine disrupters [1,2]. Therefore, routine analysis of NP in the environment is very important. Until now, chromatographic methods are currently the main ones used for the determination of NP in environmental samples, such as chromatography–ion trap tandem mass spectrometry [3,4], gas chromatography–mass spectrometry [5,6], high performance liquid chromatography-fluorescence detection [7,8], and mixed-mode high-performance liquid chromatography–electrospray mass spectrometry [9–11]. They are sensitive, but expensive apparatus and professional operators are required. By comparison, electrochemical sensor with advantages of fast response, time-saving, simple operation, low cost, and in situ analysis, has received an increasing attention. Recently, the voltammetric behaviors of NP at platinum electrode and carbon fiber electrode were reported [12,13]. However, the direct electrochemical determination of trace NP in samples is not applicable because the NP concentration is too low to be detected in the real samples. Moreover, the selectivity and sensitivity of commonly electrochemical sensors are poor.

Molecularly imprinted polymers (MIPs) are cross-linked polymers that exhibit specific binding sites for the template molecule [14]. Currently, many imprinted electrochemical sensors have been developed with specific selectivity for the template recognition [15,16]. Graphene (GP), a new fascinating nanocarbon material with one-atom thickness and a large two-dimensional plane, has attracted much attention on electrochemical sensor fabrication due to its properties of electron transfer enhancement, large surface, excellent conductivity, and super catalytic activity [17–19]. Certainly, various graphene modified sensors have been developed [20–23]. However, the commonly reported approaches for preparation of GP modified electrodes basically applying a simple assembly or sol–gel route are facing some drawbacks. Firstly, it is hard to control the thickness of the imprinted film during the imprinting film preparation, affecting the repeatability

---

Abbreviations: NP, 4-nonylphenol; FT-IR, Fourier transform infrared spectroscopy; DPV, differential pulse voltammetry; EIS, electrochemical impedance spectroscopy; MIPs, molecularly imprinted polymers; GP, graphene; GO, graphene oxide; DCC, N, N′-dicyclohexylcarbodiimide; NHS, N-hydroxysuccinimide; NP-2, polyoxyethylene (2) nonylphenyl ether; OP, octylphenol; CE, carbon electrode; GO-NH$_2$, amide group terminated graphene oxide; PPy, pyrrole polymer; RSD, recovery standard deviation.

* Corresponding author at: Key laboratory of Hunan Forest Products and Chemical Industry Engineering, Jishou University, Hunan 427000, PR China. Tel./fax: +86 743 8563911.
E-mail address: zhaohuizhang77@163.com (Z.-H. Zhang).

0039-9140/$ - see front matter Crown Copyright © 2013 Published by Elsevier B.V. All rights reserved.
http://dx.doi.org/10.1016/j.talanta.2013.04.069

of the imprinted sensors. Secondly, the GP film flaked off easily from the sensor surface when the modified sensor was immersed in the solution, which affected the stability of the modified electrode. Fortunately, many novel GP modification methods were developed to overcome these drawbacks. Recently, a feasible method anchoring carbon nanotubes on the electrode surface by use of diazonium salt reactions provides a possibility for anchoring graphene oxide (GO) onto the electrode surface [24,25]. Thus, GP modified electrode could be prepared by electrochemical reduction of amino groups terminated graphene oxide which was covalently linked onto the electrode, owing to the diazonium salt reactions between residual amino groups and the electrode. However, few papers on the electrochemical reduction of amino groups terminated graphene oxide modified imprinted electrochemical sensor were reported.

The aim of this work is to develop an imprinted electrochemical sensor based on graphene for NP determination with high sensitivity and selectivity. Amine-terminated functional graphene oxide (GO-NH_2) was covalently immobilized onto electrode by diazonium salt reactions to improve the stability and reproducibility of the modified electrode. Furthermore, graphene was prepared by electrochemical reduction of graphene oxide, enhancing the reactivity of NP and the sensitivity of imprinted electrochemical sensor. A rapid and convenient electrochemical assay for NP determination in environmental water was developed successfully.

2. Experimental

2.1. Reagents and apparatus

Graphite powder, $KMnO_4$, H_2SO_4, HCl, ethylenediamineanhydrous, potassium ferricyanide and H_2O_2 aqueous solution were all of analytical grade and were obtained from Beijing Chemical Reagents Company. N, N′-dicyclohexylcarbodiimide (DCC), N-hydroxysuccinimide (NHS), 4-Nonylphenol (NP), polyoxyethylene (2) nonylphenyl ether (NP-2) and octylphenol (OP) were obtained from Aladdin Reagents Company (Shanghai, China). 4-Nitroaniline and $NaNO_2$ were obtained from Dalian Xindie Chitin (Dalian, China). All reagents were used without further purification. Double-distilled water was used throughout the experiments.

All electrochemical experiments were carried out on a CHI 660B electrochemical workstation (Shanghai Chenhua Instrument Co. Ltd., China) using a three-electrode system, where a saturated calomel electrode (SCE) served as the reference electrode, a platinum wire electrode as the auxiliary electrode and modified carbon electrode as the working electrode. The carbon electrode was home-made with an efficient working size of $5 \times 4\ mm^2$ and the detail preparation procedure was as follows. First, acrylic-modified epoxy adhesive was used to wrap up the high purity rectangular carbon electrode brush with the size of $5 \times 4\ mm^2$ which was connected with a wire. Then the wire part was inserted through a glass tube, and the high purity rectangular carbon electrode brush part was anchored onto the glass tube formation of an impermeable device. Morphology characterization was carried out on a scanning electron microscope (JEOL, JSM-6700F) at 15 kV.

2.2. Fabrication of amide group terminated graphene oxide

Graphene oxide (GO) was prepared from purified graphite powder according to the Hummers method with minor modification [26]. The preparation procedure of amino group terminated GO is illustrated in Fig. 1. First, 300 mg GO was added into 200 mL water in a round-bottomed flask, and then sonicated for 2 h to form a homogeneous suspension for further use. After that, 2.3 g NHS and 4.16 g DCC were added into the suspension and the mixture was stirred in water bath at 50 °C for 1 h. Then, 35 mL ethylenediamine was added dropwise to the mixture and stirred with reflux for another 4 h. Finally, the reaction suspension was filtered and washed with ethanol and water several times to eliminate the residues and dried under vacuum at 50 °C.

2.3. Preparation of graphene modified electrode

Prior to modification, the bare carbon electrode (CE) was polished to a mirror using alumina slurries with 6, 1 and 0.05 μm in succession. After each polishing, the electrode was sonicated in ethanol and double-distilled water for 5 min successively to remove the adsorbed substance on the surface. Finally, it was dried under nitrogen flow.

Fig. 1 illustrates the preparation procedure of graphene modified electrode. First, a clean CE was immersed into 2.0 mL GO-NH_2 dispersion (1.0 mg mL^{-1}) in 0.5 mL HCl containing 20 mg $NaNO_2$ for 12 h. Then, the modified CE was rinsed with sufficient water to eliminate the physical adsorptive GO-NH_2. After that, GO-NH_2 which was modified on electrode (forming GP/CE) was electrochemically reduced to GP with cyclic voltammetry (CV) scanning under the potential from −0.4 to −1.4 V at 50 mV s^{-1} in 1.0 M KCl solution for three cycles. Finally, the prepared electrode was washed with water for further use.

2.4. Preparation of 4-nonylphenol imprinted graphene modified electrode

Polypyrrole was electrodeposited onto GP modified electrode to prepare NP imprinted sensor and the detailed procedures are illustrated in Fig. 1. Firstly, the modified GP/CE electrode was washed with water. Then CV scanning between 0 and 0.85 V with a scanning rate of 50 mV s^{-1} was conducted for eight cycles in the presence of 0.2 M pyrrole solution containing 5.0 mg mL^{-1} NP and 1.0 M KCl to form NP imprinted film covered on the GP/CE electrode. After deposition, the imprinted electrode was immersed into ethanol solution containing 20% of acetic acid for 1 h to remove the template molecule (form MIP/GP/CE).

3. Results and discussion

3.1. Characterization of amide group terminated graphene oxide

Amide group terminated graphene oxide (GO-NH_2) was confirmed by Fourier transform infrared spectroscopy (FT-IR). Fig. 2 shows the FT-IR spectra of GO nanosheets and GO-NH_2. The FT-IR spectrum of GO (Fig. 2a) shows a broad absorption band at 3398 cm^{-1}, which is related to the –OH groups, and absorption bands at 1623 and 1733 cm^{-1}, which are typical of carbonyl and carboxyl groups respectively, and the absorption band at 1050 cm^{-1} is the vibration of C–O, which is a characteristic group in GO. After amination, an obvious change was observed in FT-IR spectra (shown in Fig. 2b). In the spectrum of GO-NH_2, the peak at 1730 cm^{-1} disappears, and a new broad band emerges at 1626 cm^{-1} which corresponds to the C$=$O characteristic stretching band. The peak at 1535 cm^{-1} corresponds to the –NH– bending vibration, the peak at 1234 cm^{-1} corresponds to C–N stretching vibration and the peak at 641 cm^{-1} corresponds to the bending vibration of the amide group. The peaks at 892 and 1572 cm^{-1} correspond to in plane bending vibration and out-of-plane bending vibration band of the –NH_2 group respectively. The peaks at 1437, 2928 and 2850 cm^{-1} contribute to the bending vibration, the asymmetric and symmetric stretch vibration modes of C–H_2 groups, respectively. The peak at 1008 cm^{-1} corresponds to the

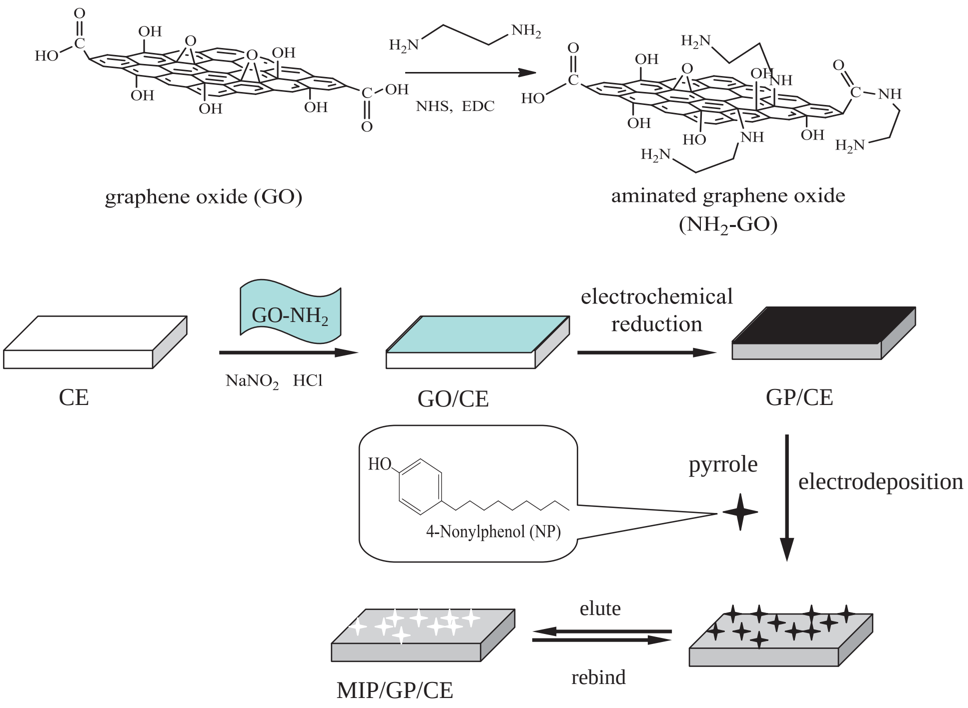

Fig. 1. Detailed procedure diagrams for fabrication of the MIP/GP/CE sensor.

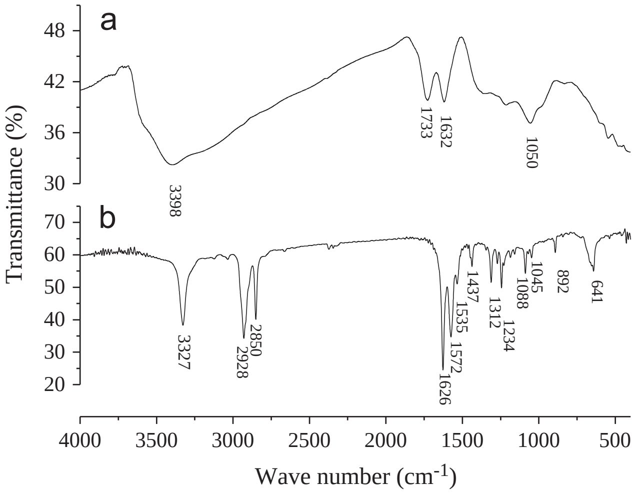

Fig. 2. FT-IR spectra of (a) graphene oxides (GO) and (b) amide group terminated graphene oxide (GO-NH_2).

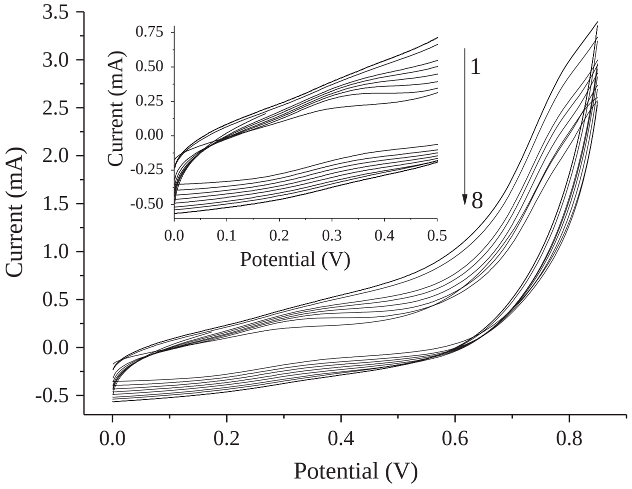

Fig. 3. Cyclic voltammogram of the electrochemical polymerization of pyrrole (0.2 M) conducted at the presence of NP (5.0 mg mL^{-1}) in 1.0 M KCl solution under scan rate of 50 mV s^{-1}.

stretching vibration of C–O band, and the peak at 1312 cm^{-1} corresponds to in plane binding stretching of –OH. These results indicated clearly that the ethylenediamineanhydrous molecules were covalently bonded to GO by the amide linkage.

3.2. Preparation and characterization of imprinted electrochemical sensor

Before preparation of the imprinted electrochemical sensor, GO-NH_2 modified on electrode was electrochemically reduced to GP (forming GP/CE) with cyclic voltammetry (CV) scanning under the potential from −0.4 to −1.4 V at 50 mV s^{-1} in 1.0 M KCl solution for three cycles. An obvious reduction current curve was observed in the first cycle, followed by greatly diminished currents in subsequent cycles during the experiment. This electrochemical behavior was similar with that of previously reported on the reduction of GO sheets [27], which validated that the reduction reaction of GO was completed (the electrode was referred as GP/CE). After that, polypyrrole (PPy) film was deposited onto the GP/CE surface with the electrodeposition method. In order to prepare NP molecularly imprinted layer on the GP/CE surface (MIP/GP/CE), cyclic voltammetry (CV) scanning in the potential of 0–0.85 V was conducted in 1.0 M KCl (pH 7.0) solution containing 0.2 M pyrrole and 5.0 mg mL^{-1} NP. Fig. 3 shows the cyclic voltammogram of pyrrole electrochemical deposition on the GP/CE surface. The peak potential of polypyrrole decreased with the increasing of the scanning cycles (as shown in Fig. 3 inset), which indicated the formation of an imprinted film on the GP/CE surface. The current decrease was caused by NP template molecules that were trapped in the polypyrrole film during the electropolymerization process, which hindered the conductivity of the polypyrrole film [28]. It is reported that a fast potential scan rate and fewer CV cycles would form a rough and poor imprinted polymer layer, and a slow potential scan rate and too many CV cycles would result in a thick and tight film in which some template molecules are entrapped too deep to be extracted [29]. So appropriate CV cycles and potential scan rate were investigated to obtain a uniform imprinted film. The results showed that the CV was conducted under the potential between 0 and 0.85 V at 50 mV s^{-1} for eight cycles to form a uniform imprinted layer on the electrode surface. Finally, the imprinted electrode was rinsed with ethanol solution containing 20% of acetic acid for 1 h to remove the template NP.

The electrochemical properties of each modification electrodes described above were investigated with the DPV technique. Fig. 4 shows the DPV of different modified electrodes in the presence of 5.0 mM $Fe(CN)_6^{3-/4-}$ PBS (pH 7.0) containing 1.0 M KCl solution. As depicted in Fig. 4a, the bare electrode shows a typical oxidation peak of $Fe(CN)_6^{3-/4-}$ at 0.20 V. After the bare electrode was covalently modified with GO by means of diazonium salt reaction of amide group terminated graphene oxide (GO-NH_2), as depicted in Fig. 4b, the peak current decreased. It was ascribed to the covering of GO-NH_2 layer on the electrode surface which acts as an insulating layer and makes the interfacial charge transfer more difficult. The electrochemical behaviors of GO-NH_2 modified electrode (GO-NH_2/CE) were similar to that of previously reported literature [29], which indicated the successful modification of amide group terminated graphene oxide onto the bare electrode. After electrochemical reduction of amide group terminated graphene oxide, forming graphene modified electrode (GP/CE), as depicted in Fig. 4c, the peak current increased, which was larger than that of bare electrode and GO-NH_2/CE. The phenomenon was attributed to the specific electronic properties and huge surface area of GP enhancing electron transfer and current value. As shown in Fig. 5d, after electrodeposition of the imprinted film, the peak current of the imprinted sensor decreased.

Electrochemical impedance spectroscopy (EIS) is an effective technique for probing the electrochemical feature of modified electrodes. For characterization of the imprinted electrode, EIS was also employed to characterize the electrochemical properties of the modified electrodes using $Fe(CN)_6^{3-/4-}$ as the redox probe in this study. The impedance spectra include a semicircle portion and linear portion. The semicircle diameter at higher frequencies corresponds to the electron-transfer resistance, and the linear part at lower frequencies corresponds to the diffusion process [30,31]. Fig. 5 represents the EIS of GP/CE (Fig. 5a), MIP/GP/CE without elution (Fig. 5b) and MIP/GP/CE (Fig. 5c) in the presence of 5.0 mM of $Fe(CN)_6^{3-/4-}$ solution. As shown in Fig. 5a, GP/CE shows a typical impedance spectrum involving the semicircle diameter at higher frequencies and a 45° liner, which indicated a solution diffusion control procedure. As shown in Fig. 5b, after an electrochemical imprinted film was electrodeposited onto the GP/CE, the semicircle diameter increased, which was ascribed to the covering of the pyrrole polymer film. When the template NP was removed from the surface of the MIP/GP/CE, the electron transfer resistance (shown in Fig. 5c) was smaller than that of MIP/GP/CE without elution, which was due to elution of the template NP molecule resulting in good conductivity. Generally, the electrode–electrolyte interface can be described as the equivalent electrical circuit in terms of a resistor and a capacitor. The impedance spectra were fitted by a simple Randle circuit with a model containing a constant phase element, and the result is shown in the inset of Fig. 5. The fitted values for the stepwise assembled layers on the electrode of electrochemical impedance spectroscopy are presented in Table 1. All the parameters include R_b (the solution resistance), R_{ct} (the electron-transfer resistance), C (the double-layer capacitance) and the Warburg impedance (W). As depicted in Table 1, GP/CE exhibits values of R_b (1.04 Ω), R_{ct} (100 Ω), C (0.35 μF) and W (0.004). After electrodeposition of polypyrrole film, the semicircle of MIP/GP/CE increased dramatically and the electron transfer resistance increased ($R_{ct}=151$ Ω) and the double-layer capacitance increased ($C=0.49$ μF). After the elution NP step was conducted, the semicircle diameter and double-layer capacitance of the imprinted electrode decreased ($R_{ct}=117$ Ω, $C=0.40$ μF). The phenomena can be explained by that after the NP template was eluted from the imprinted film, some pathways were provided,

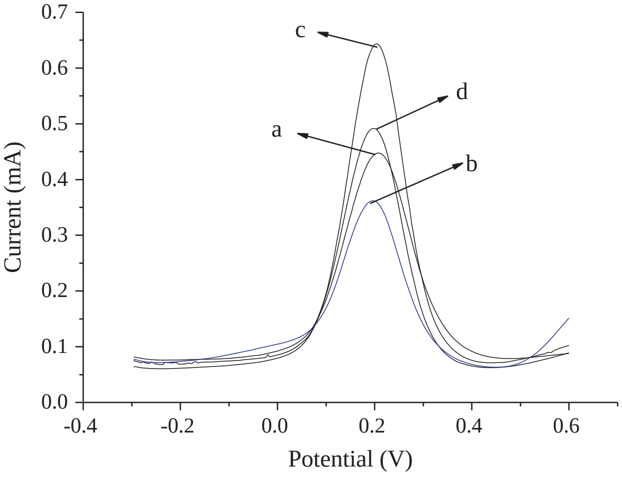

Fig. 4. DPV measurement of electrochemical conductive properties of each modification (a) the bare CE, (b) amide group terminated graphene oxide (GO-NH_2) modified electrode (GO-NH_2/CE), (c) graphene modified electrode (GP/CE) and (d) NP imprinted polypyrrole film coated graphene modified electrode (MIP/GP/CE) in the presence of 5.0 mM $Fe(CN)_6^{3-/4-}$ PBS (pH 7.0) containing 1.0 M KCl solution.

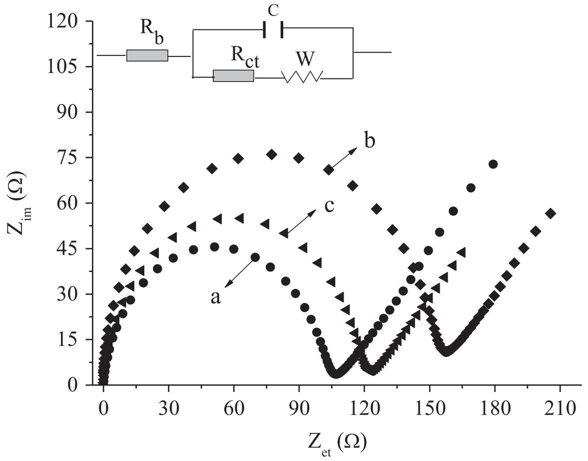

Fig. 5. Electrochemical impedance spectroscopy of (a)GP/CE, (b) MIP/GP/CE without elution and (c) MIP/GP/CE after NP is removed in the presence of 5.0 mM of Fe $(CN)_6^{3-/4-}$. Inset: equivalent electrical circuit diagrams for impedance plots, R_b (the solution resistance), R_{ct} (the electron-transfer resistance), C (the double-layer capacitance) and the Warburg impedance (the slope of the curves at a low frequency).

Table 1
Fitted impedance values of the imprinted carbon electrode.

Electrodes	R_{ct} (Ω)	C (μF)	R_b (Ω)	W
GP/CE	100	0.35	1.04	0.004
MIP/GP/CE without elution	151	0.49	1.07	0.005
MIP/GP/CE after elution	117	0.40	1.05	0.006

R_b (the solution resistance), R_{ct} (the electron-transfer resistance), C (the double-layer capacitance) and the Warburg impedance (the slope of the curves at a low frequency).

which allowed $Fe(CN)_6{}^{3-/4-}$ to diffuse through the imprinted film [28]. The above phenomena certified the preparation of the imprinted polypyrrole film successfully.

3.3. Calibration curve

A series of NP samples with different concentrations were detected in 1.0 M KCl solution with the DPV method to investigate the analytical capabilities of the developed imprinted sensor and the DPV results are recorded in Fig. 6. The blank curve current obtained in 1.0 M KCl solution without NP is 0.09 mA. As shown in Fig. 6, a strong peak current curve was observed at 0.71 V in the presence of NP, contributing to the oxidation of NP which combined with imprinted cavities. The peak currents decreased with the increasing of NP concentration. According to the previous literatures [13,28], the phenomena can be explained by that the NP template molecule combines with imprinted cavities specifically and carries out oxidation at the electrode. It was interesting that two NPs could undergo copolymerization and formation of an insulting composite which blocked the imprinting cavities. Thus, the response currents decreased with the increment of NP concentration as described in Fig. 6. It is noteworthy that the ΔIpc value (referred to the blank) exhibited a linear relationship toward the logarithmic value of NP concentrations at a range from 1.0×10^{-11} to 1.0×10^{-8} g mL^{-1} (shown in Fig. 6 inset). The linear regression equation is as follows:

$$\Delta Ipc = -0.14 \log C_{[NP]} - 0.67 \ (R^2 = 0.98).$$

The limit of detection was calculated as 3.5×10^{-12} g mL^{-1} (S/N=3). Compared with other electrochemical determination methods [28,32], the linear range and limit of detection obtained from the developed sensor in this paper were better.

3.4. Selectivity, reproducibility and stability of the MIP sensor

To evaluate the selectivity of the developed imprinted sensor, the detections of NP in the presence of foreign substances involving polyoxyethylene(2) nonylphenyl ether (NP-2) and octylphenol (OP) were conducted. Fig. 7 shows the DPV results obtained in the determination of 5.0×10^{-9} g mL^{-1} NP, 1.0×10^{-8} g mL^{-1} NP-2 and 1.0×10^{-8} g mL^{-1} OP. As shown in Fig. 7, the Ipc value toward NP was larger than that of NP-2 and OP, suggesting that the MIP/GP/CE possessed good selectivity. The lower peak currents of the MIP/GP/CE toward OP and NP-2 were attributed to the specific selectivity of the imprinted film. Briefly, the template NP molecules could combine with the imprinted cavities appropriately resulting in a strong current signal, while for the non-template NP molecule, a little current signal was obtained which is mostly attributed to the non-specific adsorption by the imprinted electrode. These results indicated the high selectivity of the imprinted electrochemical sensor.

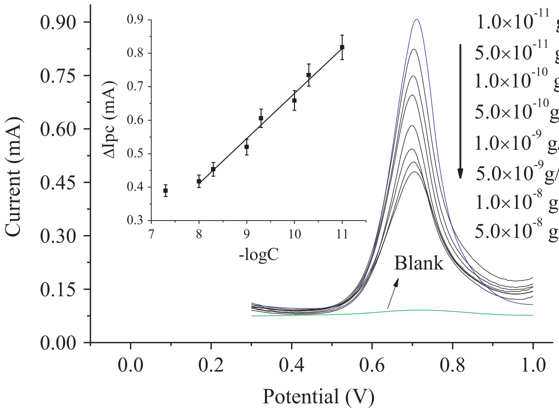

Fig. 6. Calibration curve of the imprinted electrochemical sensor toward different NP standards concentrations in 1.0 M KCl solution (inset: DPV curves).

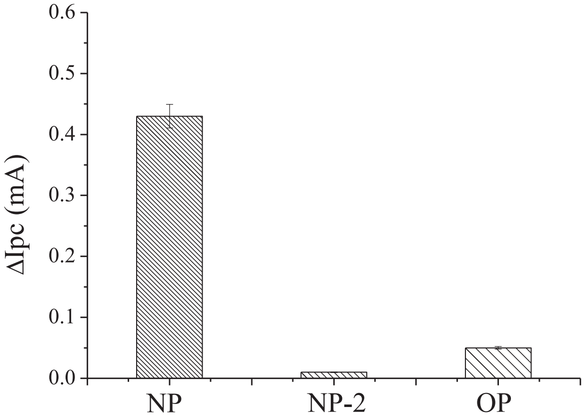

Fig. 7. DPV results of the imprinted sensor toward 1.0 ng mL^{-1} NP, 50 ng mL^{-1} NP-2 and 50 ng mL^{-1} OP in 1.0 M KCl solution.

Table 2
Results of detection NP in rain and lake water samples (n=3).

Samples	Added (ng mL^{-1})	Found (ng mL^{-1})	Recovery (%) (n=3)	RSD (%)
Rain water	1.00	0.98	98	3.1
	2.00	2.10	105	4.5
	4.00	4.08	102	4.8
Lake water	1.00	0.97	97	3.2
	2.00	2.09	105	4.0
	4.00	4.16	104	4.7

The reproducibility of the imprinted sensor was investigated by assaying 5.0×10^{-9} g mL^{-1} NP in 1.0 M KCl solution with the DVP method using three MIP sensors which were prepared under the same procedure. A recovery standard deviation (RSD) of 4.3% was obtained, indicating a good sensor-to-sensor reproducibility. The imprinted electrochemical biosensor also exhibited satisfactory stability. The experimental results showed that as much as 92% of the initial peak current was preserved after storage of the biosensor at 4 °C for 15 days.

3.5. Applications

To demonstrate its potential in practical applications, the novel imprinted sensor was applied to the detection of NP which was added in rain or lake water samples. The samples were firstly centrifuged and then filtered with a 0.45 μm membrane. After filtration, the samples were prepared with 1.0 M KCl solution, and then standard NP solution was added into 1.0 M KCl water sample. The assay of NP in different samples was conducted with the MIP/GP/NBD/CE according to the proposed method for three times. As shown in Table 2, the MIP/GP/NBD/CE was capable of detecting NP with a good average recovery of 100.3% and 100.2% for three measurements in rain and lake water, respectively, which validated the good recovery and practicability of the developed imprinted sensor.

4. Conclusions

A highly efficient molecularly imprinted electrochemical sensor platform was developed using amide group terminated graphene oxide molecules. The amide group terminated graphene oxide was characterized by FT-IR. The high sensitivity of the imprinted sensor was attributed to the large surface area and excellent electronic conductive activity of the electrochemical reduced GP modified surface. In addition, the platform offers the advantages of simplicity and efficient assay in target detection, which are essential for NP detection in environmental control. The developed electrochemical imprinted sensor was used to detect NP successfully. This work provides a general protocol to fabricate graphene modified chemical sensors with amide group terminated graphene oxide as a precursor for sensitive and selective persistent environmental pollutants detection.

Acknowledgments

This work is supported by the National Natural Science Foundation of China (Nos. 21005030, and 21267010), the Open Foundation of State Key of Chemo/Biosensing and Chemometrics (No. 212020), the Open Foundation of State Key Laboratory of Analytical Chemistry for Life Science of Nanjing University (No. SKLACL1111), the Open Foundation of Institute of Environmental Chemistry and Ecotoxicology State Key Laboratory (No. KF2011-25), the Science and Technology Innovative Research Team in Higher Educational Institutions of Hunan Province and the Construct Program of the Key Discipline in Hunan Province (No. JSU0713Z31).

References

[1] T.G. Preuss, J. Gehrhardt, K. Schirmer, A. Coors, M. Rubach, A. Russ, P.D. Jones, J. P. Giesy, H.T. Rette, Environ. Sci. Technol. 40 (2006) 5147–5153.
[2] R.J.W. Meesters, H.F. Schroöder, Anal. Chem. 74 (2002) 3566–3574.
[3] W.H. Ding, S.H. Tzing, J. Chromatogr. A 824 (1998) 79–90.
[4] C.X. Zhang, R.P. Eganhouse, J. Pontolillo, I.M. Cozzarelli, Y.X. Wang, J. Chromatogr. A 1230 (2012) 110–116.
[5] S.S. Luo, L. Fang, X.W. Wang, H.T. Liu, G.F. Ouyang, C.Y. Lan, T.G. Luan, J. Chromatogr. A 1217 (2010) 6762–6768.
[6] R. Céspedes, K. Skryjovά, M. Rakovά, J. Zeravik, M. Frάanek, S. Lacorte, D. Barceló, Talanta 70 (2006) 745–751.
[7] M. Fountoulakis, P. Drillia, C. Pakou, A. Kampioti, K. Stamatelatou, G. Lyberatos, J. Chromatogr. A 1089 (2005) 45–51.
[8] T. Tsuda, K. Suga, E. Kaneda, M. Ohsuga, J. Chromatogr. B 746 (2000) 305–309.
[9] A. Hibberd, K. Maskaoui, Z. Zhang, J.L. Zhou, Talanta 77 (2009) 1315–1321.
[10] X.L. Jin, G.B. Jiang, G.L. Huang, J.F. Liu, Q.F. Zhou, Chemosphere 56 (2004) 1113–1119.
[11] P.L. Ferguson, C.R. Iden, B.J. Brownawell, J. Chromatogr. A 938 (2001) 79–91.
[12] M.M. Ngundi, O.A. Sadik, T. Yamaguchi, S. Suye, Electrochem. Commun. 5 (2003) 61–67.
[13] H. Kuramitz, J. Saitoh, T. Hattori, S. Tanaka, Water Res. 36 (2002) 3323–3329.
[14] D. Stevenson, TrAC Trends Anal. Chem. 18 (1999) 154–158.
[15] K. Mosbach, O. Ramström, Nat. Biotechnol. 14 (1996) 163–170.
[16] A.M. Bossi, P.S. Sharma, L. Montana, G. Zoccatelli, O. Laub, R. Levi, Anal. Chem. 84 (2012) 4036–4041.
[17] L.H. Tang, Y. Wang, Y.M. Li, H.B. Feng, J. Lu, J.H. Li, Adv. Funct. Mater. 19 (2009) 2782–2789.
[18] X.S. Li, W.W. Cai, J. An, S.Y. Kim, J. Nah, D.X. Yang, R. Piner, A. Velamakanni, I. Jung, E. Tutuc, S.K. Banerjee, L. Colombo, R.S. Ruoff, Science 324 (2009) 1312–1314.
[19] K.S. Kim, Y. Zhao, H. Jang, S.Y. Lee, J.M. Kim, K.S. Kim, J.H. Ahn, P. Kim, J.Y. Choi, B.H. Hong, Nature 457 (2009) 706–710.
[20] T. Kuila, S. Bose, P. Khanra, A.K. Mishra, N.H. Kim, J.H. Lee, Biosens. Bioelectron. 26 (2011) 4637–4648.
[21] K.J. Huang, D.J. Niu, J.Y. Sun, C.H. Han, Z.W. Wu, Y.L. Li, X.Q. Xiong, Colloids Surf. B 82 (2011) 543–549.
[22] J.F. Ping, Y.X. Wang, Y.B. Ying, J. Wu, Anal. Chem. 84 (2012) 3473–3479.
[23] R.M. Iost, F.N. Crespilho, Biosens. Bioelectron. 31 (2012) 1–10.
[24] O.A. Fuentes, T. Ferri, M. Frasconi, V. Paolini, R. Santucc, Angew. Chem. Int. Ed. 123 (2011) 3519–3523.
[25] C. Cougnon, F. Gohier, D. Bélanger, J. Mauzeroll, Angew. Chem. Int. Ed. 121 (2009) 4066–4068.
[26] Y.X. Xu, K.X. Sheng, C. Li, G.Q. Shi, J. Mater. Chem. 21 (2011) 7376–7380.
[27] Z.J. Wang, X.Z. Zhou, J. Zhang, F. Boey, H. Zhang, J. Phys. Chem. C 113 (2009) 14071–14075.
[28] J.D. Huang, X.M. Zhang, S. Liu, Q. Lin, X.R. He, X.R. Xing, W.J. Lian, D. Tang, Sens. Actuators B 152 (2011) 292–298.
[29] S.G. Wu, W.G. Tan, H.H. Xu, Analyst 135 (2010) 2523–2527.
[30] H.C. Gao, F. Xiao, C.B. Ching, H.W. Duan, ACS Appl. Mater. Interfaces 3 (2011) 3049–3057.
[31] B.Y. Chang, S.M. Park, Annu. Rev. Anal. Chem. 3 (2010) 207–229.
[32] X.M. Meng, H.S. Yin, M.R. Xu, S. Ai, J.Y. Zhu, J. Solid State Electrochem. 16 (2012) 2837–2843.